Thermo-mechanical modelling of FRP cross-ply composite laminates drilling: Delamination damage analysis

Sikiru Oluwarotimi Ismail [a,*], Saheed Olalekan Ojo [b], Hom Nath Dhakal [a]

[a] *School of Engineering, University of Portsmouth, Portsmouth, England, PO1 3DJ, United Kingdom*

[b] *IMT School for Advanced Studies Lucca, Piazza San Francesco 19, 55100 Lucca, Italy*

[*] *Corresponding author*: S. O. Ismail, +44(0) 23 9284 2587, [a]sikiru.ismail@port.ac.uk

Abstract

Among other factors, thrust force, feed rate, twist drill bit chisel edge and point angle are the principal factors responsible for delamination drilling-induced damage during thermo-mechanical deformation. Hence, in this paper, an analytical thermo-mechanical model is proposed to predict critical feed rate and critical thrust force at the onset of delamination crack on CFRP composite cross-ply laminates, using the principle of linear elastic fracture mechanics (LEFM), laminated classical plate theory, cutting mechanics and energy conservation theory. The delamination zone (crack opening Mode I) is modelled as an elliptical plate. The advantages of this proposed model over the existing models in literature are that the influence of drill geometry (chisel edge and point angle) on push-out delamination are incorporated, and mixed loads condition are considered. The forces on chisel edges and cutting lips are modelled as a concentrated (point) and uniformly distributed loads, resulting into a better prediction. The model is validated with models in the literature and the results obtained show the flexibility of the proposed model to imitate the results of existing models.

Keywords: A. Laminate; B. Delamination; B. Fracture; B. Thermo-mechanical; Mixed loads condition.

1. Introduction

Fibre reinforced polymer (FRP) composite laminates possess attractive characteristics like chemical resistance, low weight, design flexibility, high strength and high stiffness-to-weight ratio [1-4]. These properties account for manufacturing of structural parts with FRP composite in the aircraft and spacecraft industries, where drilling of the structural parts is frequently encountered for manufacturing either riveted assemblies or structural repairs [1,5,6]. Due to

inherent anisotropy and structural inhomogeneity in the FRP composite laminates [3], drilling operation may cause delamination in the structural parts which in turns lowers the bearing strength and stiffness of the structure [7,8]. This consequently impair the load bearing capacity of the structure. In this context, exit-ply delamination has been identified as the most critical damage phenomenon for structural components [7,9].

Drilling takes an indispensable role among the principal machining operations which include, but are not limited to, milling, turning and boring [10]. It attracts an average of 50% of the total material removal operations [11,12]. The drilling operation is performed by a cutting tool, commonly known as a drill bit. Drill bit, such as twist drill has a multi-cutting parts with different designed complex geometry [10]. The geometric design of drills determines their efficiency and durability (tool life). Consequently, the total quality of the drilled holes depends on the geometry of the drill used. The geometric parts of drill include the point angle, chisel edge/angle, cutting lip [13-16], helix angle, diameter, and web [10]. The resultant effects of these parts are directly on the drilling variables or parameters. These parameters include, but are not limited to, drilling forces such as thrust force and torque [17], cutting force [18], cutting speed, feed rate [10], material removal rate (MRR) and depth of cut [19-21]. Among these variables, feed rate plays a crucial role in determining the quality of drilled holes of FRP composite laminates. It determines the magnitude of a thrust force during drilling operation; thrust force mainly depends on feed rate and chisel edge [22].

To eliminate the problem of delamination in drilling, calculation of the critical thrust force below which no damage occurs is important. To achieve this, classical plate theory approach is employed and assumption of linear elastic fracture mechanics (LEFM) mode I is invoked to determine the amount of work required to initiate and cause propagation of delamination drilling-induced damage in the composite laminates [5-7,9,23-27]. In an attempt to simplify calculation of the critical thrust force, many analytical models in the literature focus more on the mechanics of the FRP composite laminates while ignoring the role of drill characteristics such as drill point geometry (drill diameter, rake angle, chisel edge angle), cutting mechanism, chip formation and cutting parameters such as feed rate, among others. In addition, the effect of machining temperature which may influence drilling damage is usually not accounted for. Properties of laminate composites are usually affected by high temperature [28] and since

drilling operation is associated with thermo-mechanical deformation, a theoretical model which accounts for critical thrust force with thermal effect is desirable.

Several studies on the effect of machining parameters on force and torque prediction have been presented [29-33] and investigation based on numerical modelling has been also detailed [34,35,36]. Specifically, theoretical analysis based on hypothesis of orthogonal cut described by Langella et al. [36] reveals that the total force responsible for drilling is composed of contributions from the cutting lips and chisel edge, as illustrated in Fig. 1. This important observation assists in reconciling the disparity between concentrated and distributed load critical thrust force models in the literature [5-7] as the total thrust force can now be adequately represented by the sum of the applied force on the cutting lips and chisel edge respectively as reported by Karimi et al. [23]. Investigation shows in the work of Langella et al. [36] and Won and Dharan [37] that the thrust force due to chisel edge contribution constitutes about 60-80% at high feed rate and 40% at low feed rate, an observation which underscores the significance of the choice of feed rate in determining the critical thrust force to avoid delamination. Furthermore, from recent works in the literature, it is concluded that numerical studies on the influence of the geometric parts of drills on FRP composites drilling as the key determinants of occurrence of delamination during thermo-mechanical deformation of FRP composite laminates when subjected to drilling operation have received less attention [10,38-42].

To improve the understanding of the influence of machining parameters on delamination drilling-induced damage and in line with the realities mentioned above, based on the work of Gururaja and Ramulu [7] and Jain and Yang [22], a new thermo-mechanical formulation for the prediction of minimum critical thrust force and feed rate for analysis of delamination in composite laminates is proposed. The current formulation accounts for the total thrust force by part contributions from the cutting lips and chisel edge of the drill using the principle of superposition.
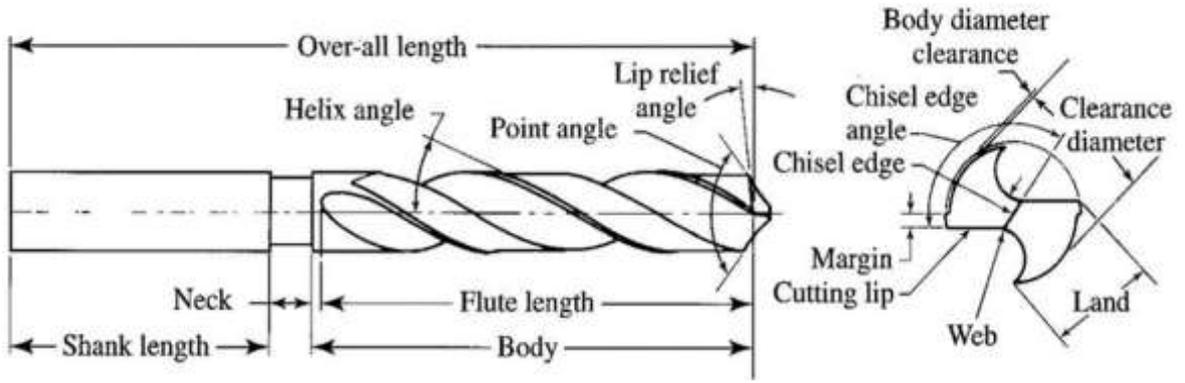
Fig. 1. A typical geometry of a double-fluted twist drill bit [10].

The proposed model allows to analyse the effect of drill point angle on the critical values of the thrust force and feed rate. To determine the relationship between the feed rate and the thrust force, the general form of the model in Langella et al. [36] is employed.

2. Model formulation

According to classical laminate theory, stress in the laminate k, as depicted in Fig. 2 may be calculated using the relation:

$$\begin{Bmatrix} \sigma_x \\ \sigma_y \\ \tau_{xy} \end{Bmatrix} = \begin{bmatrix} \underline{Q}_{11} & \underline{Q}_{12} & \underline{Q}_{16} \\ \underline{Q}_{12} & \underline{Q}_{22} & \underline{Q}_{26} \\ \underline{Q}_{16} & \underline{Q}_{26} & \underline{Q}_{66} \end{bmatrix} \left\{ \begin{Bmatrix} \epsilon^0{}_x \\ \epsilon^0{}_y \\ \gamma^0{}_{xy} \end{Bmatrix} + z \begin{Bmatrix} k_x \\ k_y \\ k_{xy} \end{Bmatrix} - \begin{Bmatrix} \alpha_x \\ \alpha_y \\ 2\alpha_{xy} \end{Bmatrix} \theta(z) \right\}, \tag{1}$$

where $\underline{Q}_{ij}$ $(i,j = 1, 2, 6)$ are the elements of the transformed stiffness matrix and $\theta(z)$ is the temperature variation along the thickness. $\epsilon^0{}_i$ $(i = x, \ y)$, $\gamma^0{}_{xy}$ and k_i $(i = x, \ y, xy)$ are the mid-plane strains and the curvature of the ply which can be expressed as:

$$\begin{Bmatrix} \epsilon^0{}_x \\ \epsilon^0{}_y \\ \gamma^0{}_{xy} \end{Bmatrix} = \begin{Bmatrix} \dfrac{\partial u^0(x,y)}{\partial x} \\ \dfrac{\partial v^0(x,y)}{\partial x} \\ \dfrac{\partial u^0(x,y)}{\partial y} + \dfrac{\partial v^0(x,y)}{\partial x} \end{Bmatrix}, \begin{Bmatrix} k_x \\ k_y \\ k_{xy} \end{Bmatrix} = \begin{Bmatrix} -\dfrac{\partial^2 w}{\partial x^2} \\ -\dfrac{\partial^2 w}{\partial y^2} \\ -2\dfrac{\partial^2 w}{\partial x \partial y} \end{Bmatrix}. \tag{2}$$

4

Here, u^0, v^0 and w are, respectively, the mid-plane displacements in the x and y directions and the deflection of the laminate ply. The resultant moments, according to classical Kirchhoff's assumption neglecting the mid-plane strains ϵ^0_x, ϵ^0_y and γ^0_{xy} are expressed as:

$$\begin{Bmatrix} M_x \\ M_y \\ M_{xy} \end{Bmatrix} = \begin{bmatrix} D_{11} & D_{12} & D_{16} \\ D_{12} & D_{22} & D_{26} \\ D_{16} & D_{26} & D_{66} \end{bmatrix} \begin{Bmatrix} k_x \\ k_y \\ k_{xy} \end{Bmatrix} - \begin{Bmatrix} M_x{}^T \\ M_y{}^T \\ M_{xy}{}^T \end{Bmatrix} ,$$

(3)

where elements of the bending stiffness matrix $[D]$ are given as:

$$D_{ij} = \sum_{k=1}^{n} \left(\frac{z_k{}^3 - z_{k-1}{}^3}{3} \right) \left(\underline{Q}_{ij}{}^k \right) .$$

If we assume a linear temperature variation through the thickness of the laminate as:

$$\theta(z) = \Delta T z ,$$

(4)

then the thermal moments can be expressed as:

$$\begin{Bmatrix} M_x{}^T \\ M_y{}^T \\ M_{xy}{}^T \end{Bmatrix} = \Delta T \sum_{k=1}^{n} \left(\frac{z_k{}^3 - z_{k-1}{}^3}{3} \right) \begin{bmatrix} \underline{Q}_{11} & \underline{Q}_{12} & \underline{Q}_{16} \\ \underline{Q}_{12} & \underline{Q}_{22} & \underline{Q}_{26} \\ \underline{Q}_{16} & \underline{Q}_{26} & \underline{Q}_{66} \end{bmatrix} \begin{Bmatrix} \alpha_x \\ \alpha_y \\ 2\alpha_{xy} \end{Bmatrix} = \Delta T \begin{bmatrix} D_{11} & D_{12} & D_{16} \\ D_{12} & D_{22} & D_{26} \\ D_{16} & D_{26} & D_{66} \end{bmatrix} \begin{Bmatrix} \alpha_x \\ \alpha_y \\ 2\alpha_{xy} \end{Bmatrix} .$$
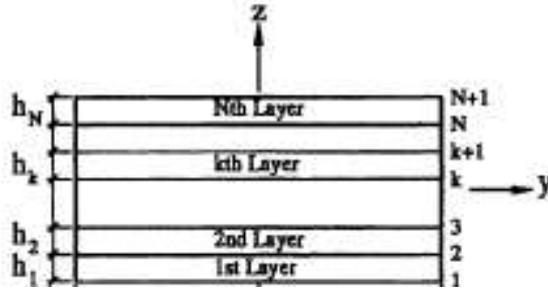
(5)

Fig. 2. Laminate geometry.

Considering a general cross-ply laminates, the bending stiffness terms $\underline{Q}_{16}$, $\underline{Q}_{26}$ are zeros. So the constitutive relation (3) becomes:

$$\begin{Bmatrix} M_x \\ M_y \\ M_{xy} \end{Bmatrix} = \begin{bmatrix} D_{11} & D_{12} & 0 \\ D_{12} & D_{22} & 0 \\ 0 & 0 & D_{66} \end{bmatrix} \begin{Bmatrix} k_x \\ k_y \\ k_{xy} \end{Bmatrix} - \begin{Bmatrix} M_x{}^T \\ M_y{}^T \\ M_{xy}{}^T \end{Bmatrix} ,$$

(6)

$$\begin{Bmatrix} M_x^T \\ M_y^T \\ M_{xy}^T \end{Bmatrix} = \Delta T \begin{bmatrix} D_{11} & D_{12} & 0 \\ D_{12} & D_{22} & 0 \\ 0 & 0 & D_{66} \end{bmatrix} \begin{Bmatrix} \alpha_x \\ \alpha_y \\ 2\alpha_{xy} \end{Bmatrix}, \tag{7}$$

where α_x and α_y are coefficients of thermal expansion in the x and y directions respectively. These coefficients follow the same transformation laws as that followed by the strain vector. Accordingly,

$$\begin{Bmatrix} \alpha_x \\ \alpha_y \\ 2\alpha_{xy} \end{Bmatrix} = \begin{bmatrix} \cos\theta^2 & \sin\theta^2 & -2\sin\theta\cos\theta \\ \sin\theta^2 & \cos\theta^2 & 2\sin\theta\cos\theta \\ \sin\theta\cos\theta & -\sin\theta\cos\theta & \cos\theta^2 - \sin\theta^2 \end{bmatrix} \begin{Bmatrix} \alpha_1 \\ \alpha_2 \\ 0 \end{Bmatrix}. \tag{8}$$

α_1 and α_2 are the coefficient of thermal expansion in the longitudinal and transverse directions of the laminate ply. According to Schapery [43], α_1 and α_2 can be expressed in terms of the matrix and fibre properties as:

$$\alpha_1 = \frac{E_f \alpha_f v_f + E_m \alpha_m v_m}{E_f v_f + E_m v_m}, \tag{9a}$$

$$\alpha_2 = (1 + v_f)\alpha_f v_f + (1 + v_m)\alpha_m v_m - \alpha_1(v_f v_f + v_m v_m), \tag{9b}$$

where E_i, α_i, v_i and v_i ($i = f, m$) are the modulus, coefficient of thermal expansion, volume fraction and Poisson's ratio of the fibre and matrix respectively.

The equilibrium equations for the thin composite plate is given as:

$$\frac{\partial^2 M_x}{\partial x^2} + 2\frac{\partial^2 M_{xy}}{\partial x \partial y} + \frac{\partial^2 M_y}{\partial y^2} + q = 0, \tag{10}$$

where $q = q_L$ is the uniformly distributed load from drilling operation and it is related to the thrust force P from the drilling machine by Zhang et al. [6]:

$$q_L = \frac{\eta P_L}{\pi a^2}, \qquad \eta = \frac{a}{b}. \tag{11}$$

P_L is the thrust force due to the distributed load, a and b denote the size of the elliptical delaminated zone along the major and minor axes as shown in Fig. 3. Substituting the constitutive relation for moments in Eq. (6) into the equilibrium Equ. (10) gives:

$$-D_{11}\frac{\partial^4 w}{\partial x^4} - 2(D_{12} + 2D_{66})\frac{\partial^4 w}{\partial x^2 \partial y^2} - D_{22}\frac{\partial^4 w}{\partial y^4} - 4D_{16}\frac{\partial^4 w}{\partial x^3 \partial y} - 4D_{26}\frac{\partial^4 w}{\partial y^3 \partial y} + \frac{4\eta P_L}{\pi a^2} = 0. \tag{12}$$

According to Zhang et al. [6], the boundary condition for the delamination zone is clamped i.e. $w = 0$, at the elliptic boundary represented by the equation, as shown in Fig. 3:

$$\frac{x^2}{a^2} + \frac{y^2}{b^2} - 1 = 0 . \tag{13}$$

The solution which satisfy the boundary equation is given as [26]:

$$w = w_0 \left(1 - \frac{x^2}{a^2} - \frac{y^2}{b^2}\right)^2 , \tag{14}$$

where w_0 is a constant to be determined.

Substituting Eq. (14) into Eq. (12) gives:

$$D_{11}w_0 + \frac{2}{3}(D_{12} + 2D_{66})\eta^2 w_0 + D_{22}\eta^4 w_0 = \frac{a^2 \eta P_L}{24\pi} . \tag{15}$$

It follows from Eq. (15) that:

$$w_0 = \frac{P_L a^2 \eta}{24\pi D^*} , \tag{16}$$

where $D^* = D_{11} + \frac{2}{3}(D_{12} + 2D_{66})\eta^2 + D_{22}\eta^4$.
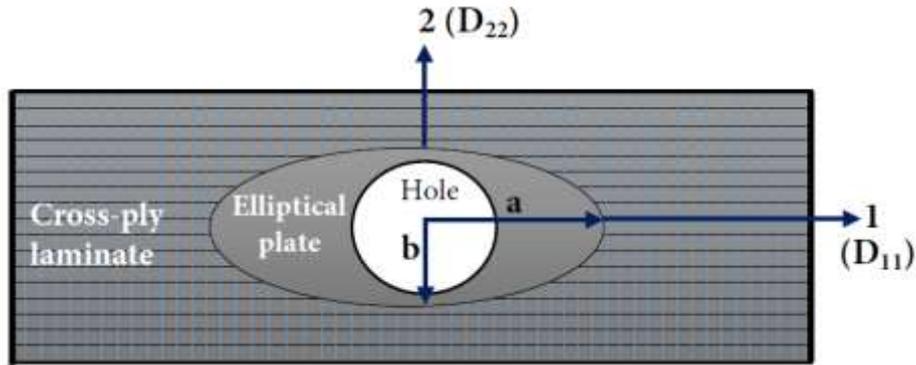

Fig. 3. Delamination zone on a cross-ply laminate modelled as an elliptical plate.

Eq. (14) can now be rewritten as:

$$w = \frac{P_L a^2 \eta}{24\pi D^*} \left(1 - \frac{x^2}{a^2} - \frac{y^2}{b^2}\right)^2 . \tag{17}$$

w in Eq. (17) is henceforth denoted as w_L to indicate deflection due to distributed load.

Based on the theorem of virtual work, the total energy balance equation for the propagation of delamination during drilling operation is expressed as:

$$\delta W = \delta U + \delta U_d \,, \tag{18}$$

where $\delta U_d = G_c \delta A$ is the energy absorbed due to delamination propagation. δA is the infinitesimal increase in the delamination area given as:

$$dA = 2\pi b \delta a \,. \tag{19}$$

δU is strain energy variation. The strain energy due to uniformly distributed load U_L is expressed as:

$$U_L = \frac{1}{2} \int \boldsymbol{\sigma} : \boldsymbol{\varepsilon} \, dV \,, \tag{20}$$

where

$$\boldsymbol{\varepsilon} = \begin{Bmatrix} \varepsilon_x \\ \varepsilon_y \\ \varepsilon_{xy} \end{Bmatrix} = \left\{ z \begin{Bmatrix} k_x \\ k_y \\ k_{xy} \end{Bmatrix} - z \begin{Bmatrix} \alpha_x \\ \alpha_y \\ \alpha_{xy} \end{Bmatrix} \Delta T \right\} \text{ and } = \begin{Bmatrix} \sigma_x \\ \sigma_y \\ \tau_{xy} \end{Bmatrix} = \begin{bmatrix} \underline{Q}_{11} & \underline{Q}_{12} & \underline{Q}_{16} \\ \underline{Q}_{12} & \underline{Q}_{22} & \underline{Q}_{26} \\ \underline{Q}_{16} & \underline{Q}_{26} & \underline{Q}_{66} \end{bmatrix} \begin{Bmatrix} \varepsilon_x \\ \varepsilon_y \\ \varepsilon_{xy} \end{Bmatrix}.$$

Expansion of Eq. (20) leads to:

$$
\begin{aligned}
U_L = \frac{1}{2} \int_{-a}^{a} \int_{-b\sqrt{1-x^2/a^2}}^{b\sqrt{1-x^2/a^2}} \int_{-z}^{z} \Big[& z^2 \underline{Q}_{11}\big(k_x{}^2 - 2k_x\alpha_x\Delta T + \alpha_x{}^2\Delta T^2\big) \\
& + {}+z^2 \underline{Q}_{22}\big(k_y{}^2 - 2k_y\alpha_y\Delta T + \alpha_y{}^2\Delta T^2\big) \\
& + 2z^2 \underline{Q}_{12}\big(k_y k_x - 2(k_y\alpha_y + k_x\alpha_x)\Delta T + \alpha_y\alpha_x\Delta T^2\big) \\
& + z^2 \underline{Q}_{66}\big(k_{xy}{}^2 - 2k_{xy}\alpha_y\Delta T + \alpha_{xy}{}^2\Delta T^2\big) \\
& + 2z^2 \underline{Q}_{16}\big(k_x k_{xy} - (k_x\alpha_{xy} + k_{xy}\alpha_x)\Delta T + \alpha_x\alpha_{xy}\Delta T^2\big) \\
& + 2z^2 \underline{Q}_{26}\big(k_y k_{xy} - (k_y\alpha_{xy} + k_{xy}\alpha_y)\Delta T + \alpha_y\alpha_{xy}\Delta T^2\big) \Big] dV
\end{aligned}
\tag{21}
$$

Evaluating the integral term over the laminate thickness gives:

$$U_L = \frac{1}{2}\int_{-a}^{a}\int_{-b\sqrt{1-x^2/a^2}}^{b\sqrt{1-x^2/a^2}}\left[D_{11}\left(k_x{}^2 - 2k_x\alpha_x\Delta T + \alpha_x{}^2\Delta T^2\right)\right.$$

$$+ D_{22}\left(k_y{}^2 - 2k_y\alpha_y\Delta T + \alpha_y{}^2\Delta T^2\right)$$

$$+ 2D_{12}\left(k_y k_x - 2\left(k_y\alpha_y + k_x\alpha_x\right)\Delta T + \alpha_y\alpha_x\Delta T^2\right)$$

$$+ D_{66}\left(k_{xy}{}^2 - 2k_{xy}\alpha_y\Delta T + \alpha_{xy}{}^2\Delta T^2\right)$$

$$+ 2D_{16}\left(k_x k_{xy} - \left(k_x\alpha_{xy} + k_{xy}\alpha_x\right)\Delta T + \alpha_x\alpha_{xy}\Delta T^2\right)$$

$$\left. + 2D_{26}\left(k_y k_{xy} - \left(k_y\alpha_{xy} + k_{xy}\alpha_y\right)\Delta T + \alpha_y\alpha_{xy}\Delta T^2\right)\right]\mathrm{d}$$

$$\tag{22}$$

Rearranging Eq. (22) gives:

$$U_L = \frac{1}{2}\int_{-a}^{a}\int_{-b\sqrt{1-x^2/a^2}}^{b\sqrt{1-x^2/a^2}}\left[D_{11}k_x{}^2 + D_{22}k_y{}^2 + 2D_{12}k_y k_x + D_{66}k_{xy}{}^2 + 2D_{16}k_x k_{xy}\right.$$

$$\left. + 2D_{26}k_y k_{xy}\right]\mathrm{dS}$$

$$- \frac{1}{2}\int_{-a}^{a}\int_{-b\sqrt{1-x^2/a^2}}^{b\sqrt{1-x^2/a^2}}\left[D_{11}k_x\alpha_x + D_{22}k_y\alpha_y + 2D_{12}\left(k_y\alpha_y + k_x\alpha_x\right)\right.$$

$$\left. + D_{66}k_{xy}\alpha_{xy} + 2D_{16}\left(k_x\alpha_{xy} + k_{xy}\alpha_x\right) + 2D_{26}\left(k_y\alpha_{xy} + k_{xy}\alpha_y\right)\right]\Delta T\,\mathrm{dS}$$

$$+ \frac{1}{2}\int_{-a}^{a}\int_{-b\sqrt{1-x^2/a^2}}^{b\sqrt{1-x^2/a^2}}\left[\bar{D}_{11} + \bar{D}_{22} + 2\bar{D}_{12} + 4\bar{D}_{16} + 4\bar{D}_{26} + 4\bar{D}_{66}\right]\Delta T^2\,\mathrm{dS}$$

$$= \frac{P_L{}^2\eta a^2}{144\pi D^*} + \frac{D'\pi a^2}{2\eta}$$

$$\tag{23}$$

$$\bar{D}_{ij} = \sum_{k=1}^{n}\left(\frac{z_k{}^3 - z_{k-1}{}^3}{3}\right)\left(\underline{Q}_{ij}{}^k\underline{\alpha}_i{}^k\underline{\alpha}_j{}^k\right) \qquad \text{for } i,j = 1,2,6 \tag{24}$$

where $D' = (\bar{D}_{11} + \bar{D}_{22} + 2\bar{D}_{12} + 4\bar{D}_{16} + 4\bar{D}_{26} + 4\bar{D}_{66})\Delta T^2$

2.1 Critical thrust force

To calculate the critical thrust force, the following assumptions are considered:

1. The uncut laminate under the drill bit exhibits an anisotropic nature.

2. The delamination zone around the exit drilled hole, with clamped boundary condition is considered elliptical.

3. Self-similar growth of the crack or inter-laminar delamination, hence the suitability of the application of LEFM approach.

4. The chisel edge force is modelled as a concentrated (point) load, while the cutting lip force is modelled as a uniformly distributed load.

The thrust force is a component of cutting (drilling) force along the drill bit axis. In accordance with Karimi et al. [23], the total thrust force for the uncut ply is accounted for by part contributions from the chisel edge and the cutting lips of the drill, as detailed in Fig. 4. Investigation shows in Won and Dharan [37] that the chisel edge force has a greater contribution than the cutting lips and is hereby modelled as a concentrated (point) load q_c while the cutting edge is modelled as a uniformly distributed load q_L. The uniformly distributed load is considered, because the downward thrust force spread out over the chisel edge and it does not pass through the centre of the drill bit during the first phase of delamination and drilling operation as a point (concentrated) load. Also, the distributed load profile has a closer agreement with the experimental results [7]. Since the linear elastic regime is considered, the total thrust force can be obtained using the law of superposition as:

$$P = P_c + P_L , \tag{25}$$

where P_c and P_L are, respectively, thrust force contributions due to concentrated and distributed loads. Let us define 2 ratios to express the relationship between P_c and P_L as:
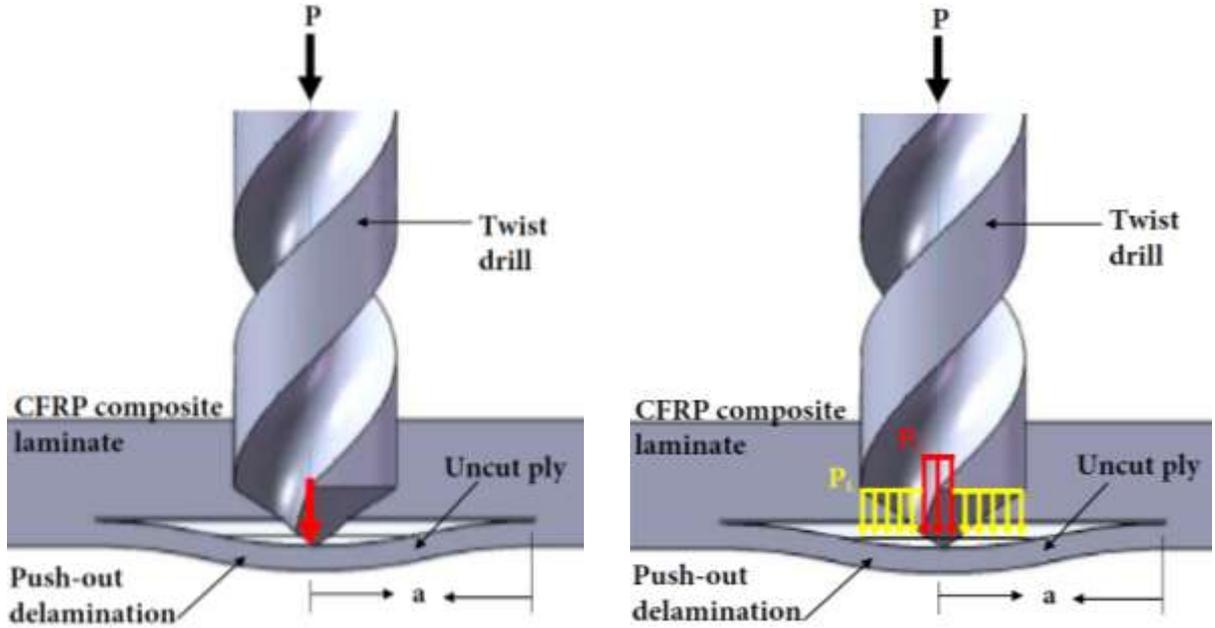
$$\alpha = \frac{P_c}{P_L}, \qquad \text{for} \geq 0 . \tag{26}$$

Using the α parameter and considering Eq. (25), the thrust forces P_c and P_L can be expressed as:

$$P_c = \left(\frac{\alpha}{1+\alpha}\right) P = \gamma P , \tag{27a}$$

$$P_L = \left(\frac{1}{1+\alpha}\right) P = (1 - \gamma)P , \tag{27b}$$

where $\gamma = \left(\frac{\alpha}{1+\alpha}\right)$ is the chisel edge ratio for $0 \leq \gamma \leq 1$.

(a) Concentrated load on chisel edge   (b) Distributed loads on chisel edge and cutting lips.

Fig. 4. Thrust force models.

The strain energy derived based on superposition principle also involves part contributions from concentrated and uniformly distributed load so that the total strain energy is given as:

$$U = U_c + U_L .$$
(28)

The expression for strain energy U_c due to concentrated load can be determined by repeating the same procedure as in Section 2 taking q in Eq. (7) as $q_c = \frac{4\eta P_c}{\pi a^2}$. Accordingly, we get:

$$w_c = \frac{P_c a^2 \eta}{6\pi D^*} \left(1 - \frac{x^2}{a^2} - \frac{y^2}{b^2}\right)^2 ,$$
(29a)

$$U_c = \frac{P_c^2 \eta a^2}{9\pi D^*} + \frac{D' \pi a^2}{2\eta} .$$
(29b)

Substituting Eqs. (23) and (29b) in Eq. (28) gives:

$$U = U_c + U_L = \frac{P_c^2 \eta a^2}{9\pi D^*} + \frac{P_L^2 \eta a^2}{144\pi D^*} + \frac{D' \pi a^2}{\eta} ,$$
(30a)

$$U = \frac{P^2 \eta a^2}{72\pi D^*} (16\gamma^2 + (1 - \gamma)^2) + \frac{D' \pi a^2}{\eta} .$$
(30b)

From Eq. (18),

$$\delta U = \frac{\partial U}{\partial a} \delta a = \left(\frac{P^2 \eta a}{72\pi D^*} (16\gamma^2 + (1-\gamma)^2) + \frac{2D'\pi a}{\eta} \right) \delta a \ . \tag{31}$$

The virtual work of external loads corresponding to the work of distributed load q_L and concentrated load q_c may be expressed as:

$$W_L = \int_{-a}^{a} \int_{-b\sqrt{1-x^2/a^2}}^{b\sqrt{1-x^2/a^2}} q_L w_L \, dxdy = \int_{-a}^{a} \int_{-b\sqrt{1-x^2/a^2}}^{b\sqrt{1-x^2/a^2}} \frac{\eta P_L}{\pi a^2} \frac{P_L a^2 \eta}{24\pi D^*} \left(1 - \frac{x^2}{a^2} - \frac{y^2}{b^2} \right)^2 dydx \ , \tag{32a}$$

$$W_c = P_c w_L (x = 0, y = 0) \ . \tag{32b}$$

Evaluating Eq. (32) gives:

$$W_L = \frac{P_L{}^2 a^2 \eta}{72\pi D^*} \ , \tag{33a}$$

$$W_c = \frac{P_c{}^2 a^2 \eta}{6\pi D^*} \ . \tag{33b}$$

The total virtual work W is now expressed as:

$$W = W_C + W_L = \frac{P^2 a^2 \eta}{72\pi D^*} (12\gamma^2 + (1-\gamma)^2) \ . \tag{34}$$

From Eq. (18),

$$\delta W = \frac{\partial W}{\partial a} \delta a = \frac{P^2 a \eta}{36\pi D^*} (12\gamma^2 + (1-\gamma)^2) \delta a \ . \tag{35}$$

Based on Eqs. (28)-(35), Eq. (18) can now be evaluated as:

$$\frac{P^2 a \eta}{36\pi D^*} (12\gamma^2 + (1-\gamma)^2) \delta a = \left(\frac{P^2 \eta a}{72\pi D^*} (16\gamma^2 + (1-\gamma)^2) + \frac{2D'\pi a}{\eta} \right) \delta a + 2G\pi b \delta a \tag{36}$$

The critical thrust force can be obtained from Eq. (36) as:

$$P^* = \frac{12\pi}{\eta} \sqrt{\frac{2D^*(D'+G_c)}{(16\gamma^2 + 2(1-\gamma)^2)}} \ . \tag{37}$$

According to Gururaja & Ramulu [7], the minimum critical thrust force corresponds to a value of $= (D_{11}/D_{22})^{\frac{1}{4}}$, as shown in Fig. 3. With this realization, Eq. (37) becomes:

$$P^* = 12\pi \left(\frac{D_{11}}{D_{22}} \right)^{\frac{1}{4}} \sqrt{\frac{2D_c{}^*(D'+G_c)}{(16\gamma^2 + 2(1-\gamma)^2)}} \ , \tag{38}$$

where $D_c{}^* = 2D_{11} + \frac{2}{3}(D_{12} + 2D_{66})\left(\frac{D_{11}}{D_{22}}\right)^{\frac{1}{2}}$.

Eq. (38) gives the minimum critical thrust force below which delamination will not occur. Based on the model Eq. (38), the total thrust force is bounded as unit of the sum of P_L and P_c.

2.2 Effect of point angle (ε)

It is remarked here, according to Langella et al. [36], that the point angle ε significantly affects the thrust force and analysis of total thrust force due to contributions of the cutting lips and the chisel edge shows that the risk of material damage during drilling increases proportionally to the feed rate and point angle. For a drill with an arbitrary point angle, Eq. (25) becomes:

$$P(\varepsilon) = P_c(\varepsilon) + P_L(\varepsilon). \tag{39}$$

$P_c(\varepsilon)$ and $P_L(\varepsilon)$ according to Won and Dharan [37] is given by:

$$P_L(\varepsilon) = \frac{k_L(\varepsilon)}{\exp(\alpha_L \gamma_L)}\sqrt{f}, \tag{40a}$$

$$P_c(\varepsilon) = \frac{k_c(\varepsilon)}{\exp(\alpha_c \gamma_c)}\sqrt{f}. \tag{40b}$$

where γ_L and γ_c are the average rake angle and the chisel edge rake angle. k_L and k_c are parameters related to specific energies at the cutting lips and chisel edge respectively and can be determined by means of a single test described in Langella et al. [36].

$$\alpha_L = 1.089 \ln 10 = 2.51. \tag{41}$$

With respect to the procedure described in Langella et al. [36], it is remarked that the mechanistic model (40) is best suited for drills with 160^0 point angle. Using this as a reference point angle ε_0, Eq. (39) can be rewritten as:

$$P(\varepsilon_0) = P_c(\varepsilon_0) + P_L(\varepsilon_0). \tag{42}$$

Considering the relationship between chisel edge and cutting lips thrust forces and the total thrust force in Eq. (27), the chisel edge and cutting lips thrust forces for a drill with an arbitrary point angle ε can be written in terms of the total thrust force P as:

13

$$P_c = \gamma^\beta P \,, \tag{43a}$$

$$P_L = \left(1 - \gamma^\beta\right)P \,, \tag{43b}$$

where $\beta = \frac{\varepsilon}{\varepsilon_0}$ is the ratio between the arbitrary point angle ε and the reference point angle ε_0.

Given Eq. (43), and repeating the procedure in Section 2.1, the equation for the critical thrust force is given as:

$$P^* = 12\pi \left(\frac{D_{11}}{D_{22}}\right)^{\frac{1}{4}} \sqrt{\frac{2D_c{}^*(D'+G_c)}{\left(16\gamma^{2\beta}+2\left(1-\gamma^\beta\right)^2\right)}} \,. \tag{44}$$

2.3 Feed rate

Feed rate plays a vital role in determining delamination. Thrust force is a function of feed rate. Therefore, emphasis must be placed on feed rate because it can be controlled as an input and independent drilling parameters, unlike thrust force. Since the total thrust force is a sum of contributions due to the cutting lips and the chisel edge, the relationship between the critical thrust force and the critical feed rate can be obtained based on Eqs. (39)-(40) and (43) as:

$$P^* = \frac{k_c}{\exp(\alpha_c\gamma_c)}\sqrt{f^*} + \frac{k_L}{\exp(\alpha_L\gamma_L)}\sqrt{f^*} \,. \tag{45}$$

Substituting for P^* in Eq. (42), the critical feed rate is expressed as:

$$f^* = \frac{144\pi^2}{\varphi^2}\left(\frac{D_{11}}{D_{22}}\right)^{\frac{1}{2}}\left[\frac{2D_c{}^*(D'+G_c)}{\left(16\gamma^{2\beta}+2\left(1-\gamma^\beta\right)^2\right)}\right], \tag{46}$$

where $\varphi = \frac{k_c}{\exp(\alpha_c\gamma_c)} + \frac{k_L}{\exp(\alpha_L\gamma_L)}$.

3. Results and discussion

To demonstrate the effect of drill characteristics on the delamination of the FRP composite, a cross-ply laminate sequence consisting of 16 plies with material properties detailed in Table 1 is considered. Delamination is assumed to occur when the laminate is drilled so that there are n uncut plies below the drilled hole. Effect of drill characteristics (chisel edge and point

angle ratios) on the critical thrust force and the critical feed rate are analysed and comparison of the proposed model with other models in the literature are also demonstrated. The underlying assumption in the analysis of the point angle is that the dependence of the critical thrust force is significant when the total thrust force is composed of part contributions due to the cutting lips and the chisel edge.

Table 1

The material properties of the CFRP cross-ply composite laminates.

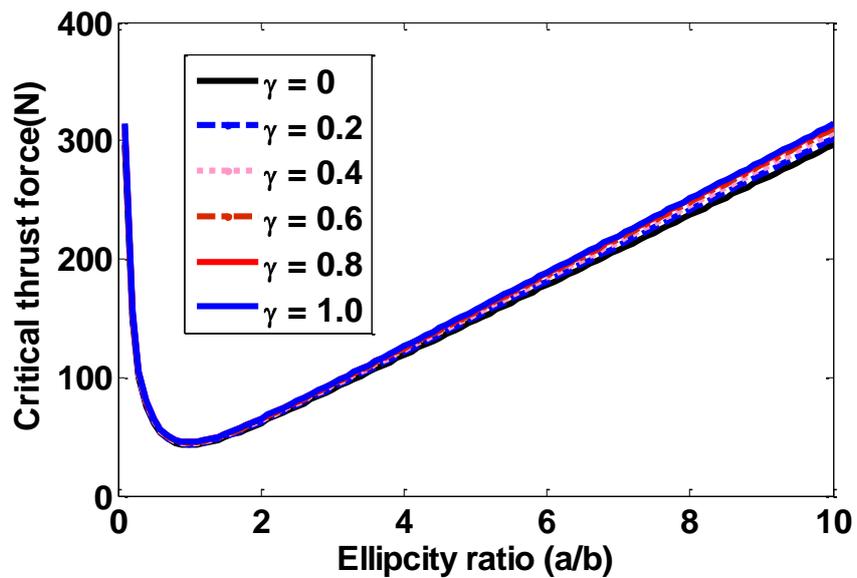| Material	E_1 (MPa)	E_2 (MPa)	v_{12}	G_{12} (MPa)	α_1 (10^{-6}/K)	α_2 (10^{-6}/K)	G_{IC} (N/mm)	h (mm)
CFRP	175.9	8.1	0.32	4.4	-0.07	30.9	0.328	0.3125

Fig. 5. Ellipticity ratio effect on minimum critical thrust force.

The critical thrust force is a function of ellipticity ratio according to Eq. (37). Additionally, the effect of ellipticity ratio η of the critical thrust force is shown in Fig. 5 where it is inferred that the ellipticity ratio for which the critical thrust force is minimum must be less than 1 for a range of values of chisel edge ratio, γ. At this minimum value, the possibility of delamination is quite lower. Meanwhile, immediately after ellipticity ratio of 1, ellipticity (delamination zone) increases with the critical thrust force, implies increase in delamination damage.

Analysis of the effect of chisel edge ratio on the minimum critical thrust force in Fig. 6 shows that the critical thrust force increases to a peak and then reduces with increasing chisel edge ratio. For a fixed value of the chisel edge ratio, the critical thrust force increases with increasing point angle ratio and this effect is more profound at low chisel edge ratio. This is an important observation since it underscores the significance of the point angles for a specific drilling operation and also confirms the findings in Langella et al. [36]. Both Figs. 6 and 7 depict that effective control and selection of the drill bit geometrical parameters (reduced chisel edge and point angle) could enhance possibility of delamination-free drilling of CFRP composite laminates using higher feed rate and thrust force.
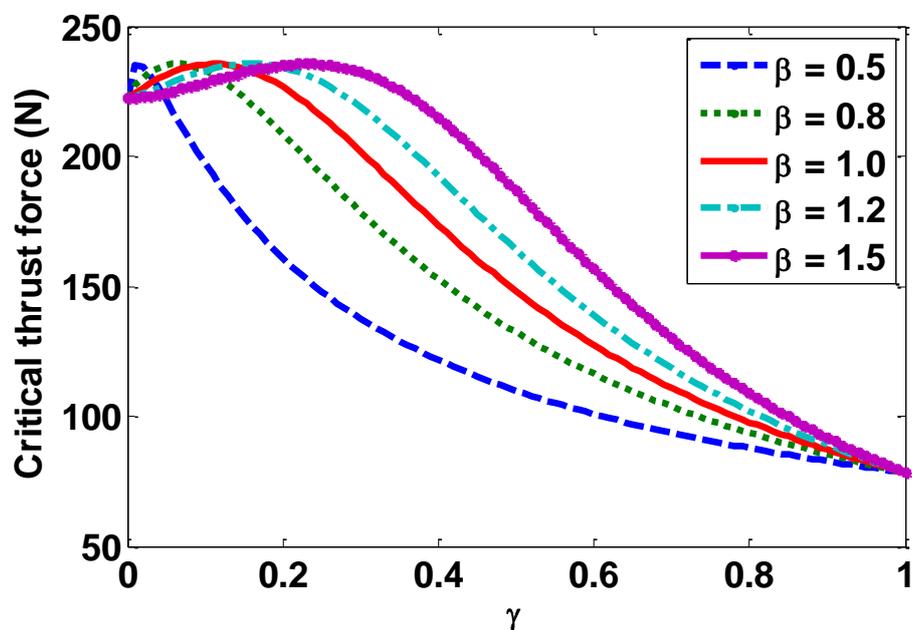

Fig. 6. Effect of chisel edge load on minimum critical thrust force for different point angles.

Furthermore, it is observed in Fig. 7 that critical feed rate dependence on the chisel edge ratio and the point angle ratio keeps the same profile like the critical force. This is expected since there is a direct proportional relationship between the thrust force and the feed rate.
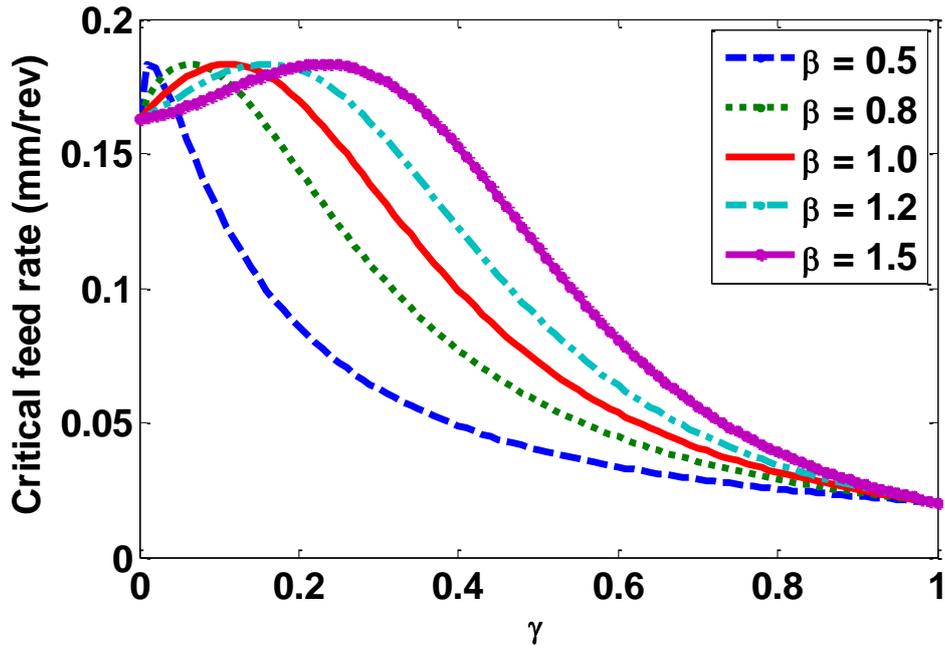
Fig. 7. Effect of chisel edge load on critical feed rate for different point angles ($\varphi = 550$ N rev/mm).

During experimental drilling of FRP composite laminate, the critical thrust force increases rapidly as the drill bit tends to gain entry into the laminate at inception. It increases to a peak before a steady state condition is maintained at full engagement of the drill inside the laminate, with nearly half number of the total plies. Immediately after this state, the drill bit approaches the exit side of the hole at a decreasing number of uncut plies, the critical thrust force is drastically reduced. The results obtained and presented in Fig. 8 unambiguously supports this drilling phenomenon [44].

Moreover, feed rate can be related with the thrust force (Figs. 7 and 8). This may be necessary in order to facilitate direct programming of feed rate into the CNC machine centre, to predict the thrust force towards having delamination-free composite drilling. This is possible because thrust force depends on feed rate. Meanwhile, the concerned feed rate is a function of feed per revolution (mm/rev), not a linear feed rate in inches per minute (''/min). Summarily, it is evident that a lower thrust force is function of a lower feed rate; the thrust force increases with the feed rate.
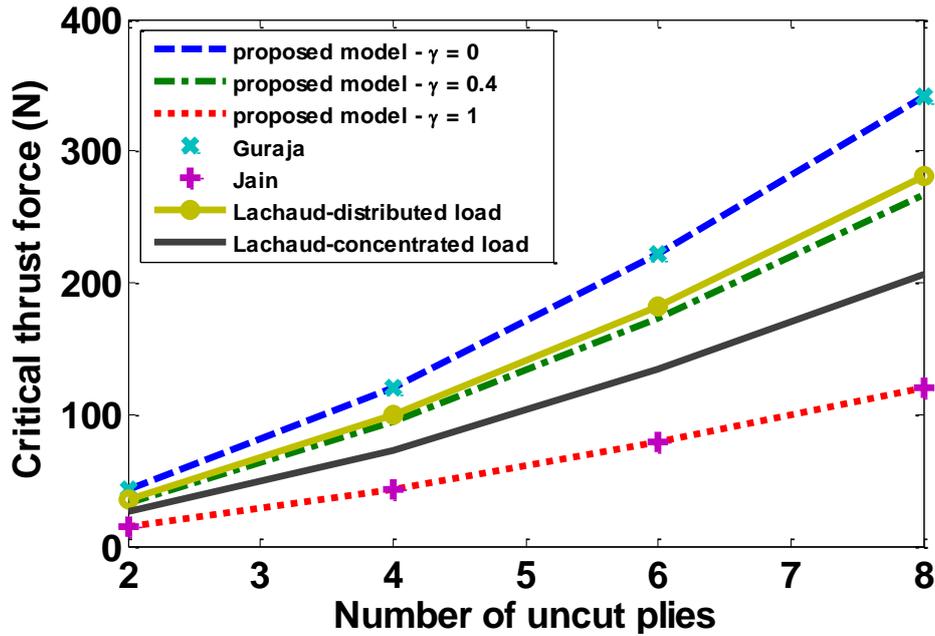
Fig. 8. Minimum critical thrust force for different models and the proposed model.

Neglecting the effect of temperature, the proposed model captures contributions of distributed and concentrated loads with limiting values approaching Gururaja and Ramulu [7] distributed load model for $\gamma = 0$ on one hand and Jain and Yang [22] concentrated load model for $\gamma = 1$ on the other hand, as depicted in Fig. 8. Also, it is observed from Fig. 8 that behavioural increase of the predicted critical thrust force as the number of the uncut ply increases. It is evident that at low number of the uncut ply, especially at 2, all the models have a very close values of predicted critical thrust forces. The proposed model with $\gamma = 0$ predicts the Gururaja and Ramulu [7] model exactly. On this basis, the model proposed in this work is validated against existing models in the literature and specifically, Lachaud et al. [5] distributed and concentrated load models is compared with the proposed model with varying chisel edge ratio. It is shown in Fig. 8 that with $\gamma = 0.4$, the result for the proposed model approaches the Lachaud et al. [5] distributed load model, an observation which signifies the flexibility of the proposed model based on chisel edge contribution to the total thrust force. In addition, the proposed model with $\gamma = 0.4$ predicts lower critical thrust force than the Lachaud et al. [5] and Gururaja and Ramulu [7] distributed models.

4. Conclusions

A new thermo-mechanical model for the prediction of critical thrust force and critical feed rate has been proposed in this work. The new model takes into account the effect of drill

characteristics such as the chisel edge load and the point angle. It also detailed the thermal effect of the drilling operation. Essentially, the proposed model is formulated based on part contributions of distributed load by the cutting lips of the drill and concentrated load by the drill chisel edge. This mixed load condition allows for the introduction of point angle variable which is a novelty with respect to existing models in the literature. Analysis of the results show that with increasing chisel edge ratio, the critical thrust force and the feed rate increase to a peak and then approach the limiting value of the thrust force and feed rate for a concentrated load condition. The model is validated with models in the literature and the results show the flexibility of the model to imitate the results of existing models. A future development is to validate the proposed model with experimental drilling operation which is strongly characterized by thermo-mechanical deformation.

Acknowledgements

References

[1] Singh AP, Sharma M, Singh I. A review of modelling and control during drilling of fibre reinforced plastic composites. Compos Part B Eng 2013;47:118-25.

[2] Wu T, Zhang K, Cheng H, Liu P, Song D, Li Y. Analytical modelling for stress distribution around interference fit holes on pinned composite plates under tensile load. Compos Part B Eng 2016;100:176-85.

[3] Chebbi E, Wali M, Dammak F. An anisotropic hyperelastic constitutive model for short glass fibre-reinforced polyamide. Int J Eng Sci 2016;106:262–72.

[4] Mohammadabadi M, Daneshmehr AR, Homayounfard M. Size-dependent thermal buckling analysis of micro composite laminated beams using modified couple stress theory. Int J Eng Sci 2015;92:47–62.

[5] Lachaud F, Piquet R, Collombet F, Surcin L. Drilling of composite structures. Compos Struct 2001;52(3-4):511-6.

[6] Zhang LB, Whang LJ, Liu XY. A mechanical model for predicting critical thrust forces in drilling composite laminates. Proc Inst Mech Eng Part B: J Eng Manuf 2001;215(2):135-46.

[7] Gururaja S, Ramulu M. Modified exit-ply delamination model for drilling FRPs. J Compos Mater 2009;43(5):483-500.

[8] Tagliaferri V, Caprine G, Diterlizzi A. Effect of drilling parameters on the finish and mechanical properties of GFRP composites. Int J Mach Tools Manuf 1990;30(1):77-84.

[9] Saoudi J, Zitoune R, Gururaja S, Mezlini S, Hajjaji AA. Prediction of critical thrust force for exit ply delamination during drill composite laminates: thermo-mechanical analysis. Int J Machin Machinab Mater 2016;18(1-2):77-98.

[10] Ismail SO, Dhakal HN, Dimla E, Popov I. Recent advances in twist drill design for composites machining: A critical review. Proc Inst Mech Eng Part B: J Eng Manuf 2016:1-16.

[11] Isbilir O, Ghassemieh E. Finite element analysis of drilling of titanium alloy. Procedia Eng 2011;10:1877–82.

[12] Yang Y, Sun J. Finite element modelling and simulating of drilling of titanium alloy. Proceedings of the Second International Conference on Information and Computing Science, IEEE Computer Society. Manchester, May, 2009. p. 178-81.

[13] Heisel U, Pfeifroth T. Influence of point angle on drill hole quality and machining forces when drilling CFRP. Procedia CIRP 2012;1:471-76.

[14] Sambhav K, Tandon P, Dhande SG. Geometric modelling and validation of twist drills with a generic point profile. Appl Math Model 2012;36(6):2384–403.

[15] Paul A, Kapoor SG, DeVor RE. Chisel edge and cutting lip shape optimisation for improved twist drill point design. Int J Mach Tools Manuf 2005;45(4-5):421–31.

[16] Ahmadi K, Savilov A. Modeling the mechanics and dynamics of arbitrary edge drills. Int J Mach Tools Manuf 2015;89:208–20.]

[17] Feito N, Diaz-Álvarez J, López-Puente J, Miguélez MH. Numerical analysis of the influence of tool wear and special cutting geometry when drilling woven CFRPs. Compos Struct 2016;138:285–94.

[18] Arola D, Ramulu M. Orthogonal cutting of fibre-reinforced composites: A finite element analysis. Int J Mech Sci 1997;39(5):597-13.

[19] Harris SG, Doyle ED, Vlasveld AC, Audy J, Quick D. A study of the wear mechanisms of Ti1-xAlxN and Ti1-x-yAlxCryN coated high-speed steel twist drills under dry machining conditions. Wear 2003;254(7-8):723–34.

[20] Webb PM. Dynamics of the twist drilling process. Int J Prod Res 1993;31(4):823–8.

[21] Xiong L, Fang N, Shi H. A new methodology for designing a curve-edged twist drill with an arbitrarily given distribution of the cutting angles along the tool cutting edge. Int J Mach Tools Manuf 2009;49(7-8):667–77.

[22] Jain S, Yang DCH. Effect of feed rate and chisel edge on delamination in composite drilling. J Eng Ind 1993;115(4):398-405.

[23] Karimi NZ, Heidary H, Minak G. Critical thrust and feed prediction models in drilling of composite laminates. Compos Struct 2016;148:19–26.

[24] Ko¨nig W, Wulf Ch, Grass P, Willerscheid H. Machining of fibre-reinforced plastics. CIRP Annals-Manuf Technol 1985;34(2):537–48.

[25] Upadhyay PC, Lyons JS. On the evaluation of critical thrust for delamination-free drilling of composite laminates. J Reinf Plast Compos 1999;18(14):1287-303.

[26] Timoshenko S, Woinowsky-Krieger S. Theory of Plates and Shells. New York: McGraw-Hill, 1959.

[27] Jones RM. Mechanics of Composite Materials. Washington D.C.: McGraw-Hill, 1975.

[28] Ojo SO, Paggi M. Thermo-visco-elastic shear-lag model for the prediction of residual stresses in photovoltaic modules after lamination. Compos Struct 2016;136:481-92.

[29] Bhattacharyya D, Horrigan DPW. A study of hole drilling in kevlar composites. Compos Sci Technol 1998;58(2):267-83.

[30] Dillio A, Paoletti A, Veniali F. Process in drilling of composites. In: Proceedings of composite materials symposium. Chicago, 1992. p. 199-203.

[31] Miller JA. Drilling graphite/epoxy at Lockheed. Amer Mach Autom Manuf 1987;131(10):70-1.

[32] Chen WC. Some experimental investigation in the drilling of carbon fibre reinforced plastics (CFRP) composite laminates. Int J Mach Tools Manuf 1997;37(8):1097-108.

[33] Khashaba UA, El-Sonbaty IA, Selmy AI, Megahedv AA. Machinability analysis in drilling woven GFR/epoxy composites: Part II – Effect of drill wear. Compos Part A: Appl Sci Manuf 2010;41(9):1130–7.

[34] Chandrasekharan V, Kapoor SG, DeVor RE. A mechanistic approach to predicting the cutting forces in drilling: with application to fibre-reinforced composite materials. J Eng Ind 1995;117(4):559–70.

[35] Chandrasekharan VA. A model to predict the three-dimensional cutting force system for drilling with arbitrary point geometry. PhD Thesis, University of Illinois at Urbana-Champaign, United States 1996.

[36] Langella A, Nele L, Maio AA. A torque and thrust prediction model for drilling of composite materials. Compos Part A: Appl Sci Manuf 2005;36(1):83–93.

[37] Won MS, Dharan CKH. Chisel edge and pilot hole effects in drilling composite laminates. J Manuf Sci Eng 2002;124(2):242–7.

[38] Ismail SO, Dhakal HN, Dimla E, Beaugrand J, Popov I. Effects of drilling parameters and aspect ratios on delamination and surface roughness of lignocellulosic HFRP composite laminates. J Appl Poly Sci 2016;133(7):1-8.

[39] Soldani X, Santiuste C, Muñoz-Sánchez A, Miguélez MH. Influence of tool geometry and numerical parameters when modelling orthogonal cutting of LFRP composites. Compos Part A: Appl Sci Manuf 2011;42(9):1205–16.

[40] Abele E, Fujara M. Simulation-based twist drill design and geometry optimization. CIRP Annals - Manuf Technol 2010; 59(1):145–50.

[41] Wang J, Zhang Q. A study of high-performance plane rake faced twist drills. Part I: Geometrical analysis and experimental investigation. Int J Mach Tools Manuf 2008;48(11):1276-85.

[42] Audy J. A study of computer-assisted analysis of effects of drill geometry and surface coating on forces and power in drilling. J Mater Process Technol 2008; 204(1-3):130–8.

[43] Schapery RA. Thermal expansion coefficients of composite materials based on energy principles. J Compos Mater 1968;2(3):380-404.

[44] Ismail SO, Dhakal HN, Popov I, Beaugrand J. Comprehensive study on machinability of sustainable and conventional fibre reinforced polymer composites. Eng Sci Technol, int J 2016:1-10 (in press).